Journal of Cellular Biochemistry 97:519–529 (2006)

# Interleukin-1β Induces Osteopontin Expression in Pulmonary Fibroblasts

**David M. Serlin,[1]* Ping Ping Kuang,[1] Mangalalaxmy Subramanian,[1] Anthony O'Regan,[3] Xinfang Li,[1] Jeffrey S. Berman,[1,2] and Ronald H. Goldstein[1,2]**

[1]Department of Medicine, Pulmonary Center, Boston University School of Medicine, Boston, Massachusetts
[2]Department of Medicine, Division of Pulmonary Medicine, Boston VA Healthcare System, Boston, Massachusetts
[3]Respiratory Medicine, University College Hospital, Galway, Ireland

**Abstract** Osteopontin is a multifunctional matricellular protein identified as one of the most upregulated genes in pulmonary fibrosis. Experimental animal models have identified early pro-fibrotic cytokines as essential to the pathogenesis of inflammation-induced pulmonary fibrosis. However, the principal sources of osteopontin in the fibroproliferative lung, and the factors responsible for its induction, have not been fully defined. We isolated primary rat lung fibroblasts in culture to examine the expression and regulation of lung fibroblast-derived osteopontin. Our results demonstrate a potent and dramatic increase in osteopontin expression induced by interleukin-1β (IL-1β), whereas tumor necrosis factor-α, transforming growth factor-β, and angiotensin II had minimal effect. Stimulation with IL-1β resulted in the secretion of soluble osteopontin protein. We found that osteopontin expression by IL-1β was regulated via signaling primarily through the mitogen-activated protein kinase member ERK1/2, partially by p38 MAPK, but not at all by JNK. Finally, the mechanism of IL-1β increase in osteopontin mRNA requires de novo transcription and translation. In conclusion, we find that osteopontin is expressed by primary lung fibroblasts and is potently upregulated by the early inflammatory and pro-fibrotic cytokine IL-1β. Activated fibroblasts may be a significant source of osteopontin production during lung fibrogenesis. J. Cell. Biochem. 97: 519–529, 2006. 

**Key words:** osteopontin; interleukin-1β; lung; fibroblast

Osteopontin is a multifunctional matricellular protein markedly upregulated in pulmonary fibrosis [Zuo et al., 2002]. It is a highly glycosylated phosphoprotein possessing an arginine-glycine-aspartate (RGD) integrin domain, heparin binding motifs, and cleavage sites for thrombin and matrix metalloproteinases (MMP)-3 and -7 [O'Regan et al., 2000]. Intracellular and extracellular forms of osteopontin have been identified [Zohar et al., 2000], with the extracellular protein functioning as a pro-inflammatory and pro-fibrotic cytokine [O'Regan, 2003]. Osteopontin-deficient transgenic mice demonstrate altered wound healing in the skin, heart, and lung [Liaw et al., 1998; O'Regan et al., 2001; Trueblood et al., 2001]. After bleomycin pulmonary injury, osteopontin-deficient mice develop abnormal extracellular matrix deposition and lung remodeling, characterized by enlarged cystic airspaces, reduced type-I collagen production, and decreased levels of activated MMP-2 and transforming growth factor-β (TGF-β) [Berman et al., 2004]. In vitro, osteopontin is both chemotactic and mitogenic for fibroblasts [Takahashi et al., 2001]. It can induce fibroblast-collagen gel contraction, thus augmenting cell–matrix interactions [Ashizawa et al., 1996].

Little is known about the factors that regulate osteopontin expression during organ fibrogenesis. After tissue injury, inflammatory cytokines are generated that are essential for proper wound healing. Specifically, over-production of the cytokines IL-1β, tumor necrosis factor-α

Grant sponsor: NIH/NHLBI; Grant numbers: F32-HL71388, R01-HL63339, R01-HL70182, P01-HL46902.

*Correspondence to: David M. Serlin, MD, Pulmonary Center, Boston University School of Medicine, 715 Albany Street, R304, Boston, MA 02118. E-mail: daserlin@bu.edu

Received 15 April 2005; Accepted 22 August 2005

DOI 10.1002/jcb.20661

(TNF-α), TGF-β as well as osteopontin have all been implicated in the pathogenesis of organ fibrosis. In the kidney following glomerular injury, osteopontin expression increases within the sclerotic crescents and thickened interstitium [Lan et al., 1998; Persy et al., 2003]. Pretreatment with a soluble IL-1 receptor antagonist decreases osteopontin expression and abrogates renal injury [Yu et al., 1999]. In the heart, myocardial injury leads to increased fibroblast-associated osteopontin and its expression is dependent upon the pro-fibrotic peptide angiotensin II (AII) [Ashizawa et al., 1996]. Finally, bleomycin-lung injury and transgenic mice overexpressing TNF-α both develop increased osteopontin expression in the lung temporally related to the onset of fibrosis [Miyazaki et al., 1995; Takahashi et al., 2001]. Whether fibroblasts within the lung produce osteopontin, and which mediators might be responsible for its regulation, remains unknown.

We hypothesize that the inflammatory cytokines generated after lung injury induce osteopontin expression by pulmonary fibroblasts. In these studies, we demonstrate for the first time osteopontin mRNA and protein expression by primary pulmonary fibroblasts. We show the potent and specific induction of osteopontin by the inflammatory and pro-fibrotic cytokine IL-1β. Finally, we find that the mitogen-activated protein kinase (MAPK) signaling pathways are required for IL-1β-induced expression of osteopontin in primary lung fibroblasts.

## MATERIALS & METHODS

### Cell Culture

Neonatal rat pulmonary fibroblasts, or lung interstitial cells (LIC), were isolated from 3-day-old Sprague–Dawley rats (Charles River Breeding Laboratory, Wilmington, MA) as previously described [Carreras et al., 2001]. We have extensively characterized rat LIC under various conditions, most recently after IL-1β treatment [Kuang and Goldstein, 2003]. Rat LIC are preferable to mouse cells in their ease of acquisition and lack of strain differences that confound murine cell-based experiments. Cultured LIC at passage 2 or 3 were seeded in 6-well tissue culture plates (Costar-Corning Life Sciences, Acton, MA) at a density of $5 \times 10^5$/well in complete medium (minimal essential medium (MEM) plus 1 mM penicillin and streptomycin, all from Invitrogen) plus 10% fetal bovine serum (FBS, HyClone, Logan, UT). Cells were maintained in a humidified 5% $CO_2$ incubator at 37°C. Confluent cultures were rendered quiescent by changing the medium to 0.5% FBS-MEM for 24 to 48 h and replaced with fresh 0.5% FBS-MEM 12 h prior to treatment. For assessment of secreted osteopontin protein, and for TGF-β treatment, medium was changed to 0% FBS-MEM in the experimental conditions. Rat LIC were treated with the cytokines IL-1β (0.025–0.5 ng/ml), TNF-α (1–20 ng/ml), and TGF-β (10 ng/ml) (all from R&D, Minneapolis, MN) and $10^{-6}$ M of Angiotensin II (Sigma) for 24 h. The soluble IL-1 receptor antagonist (sIL-1ra, 150 ng/ml, R&D) and small chemical inhibitors U0126, PD98059, SB203580, and JNK inhibitor-I (all 10 μM, Calbiochem San Diego, CA) were added to the cell cultures 30 min prior to IL-1β treatment. Cycloheximide (10 μg/ml) and actinomycin-D (1 μg/ml, both from Sigma) were added to fibroblast cultures one hour prior to IL-1β treatment.

### RNA Isolation and Analysis

Total RNA from cultured rat LIC was isolated using TRIzole reagent (Invitrogen) per the manufacturer's protocol and analyzed by Northern blotting. Non-radioactive RNA probes were generated from sequence-specific cDNA clones. Poly-A mRNA from rat neonatal fibroblasts was reverse-transcribed (Promega, Madison, WI) to generate cDNA. Rat osteopontin specific cDNA was then amplified by polymerase chain reaction (PCR) using TaKaRa Ex Taq (Takara Bio, Japan) and custom primers for rat osteopontin (5′ end: ATGAGACTGGCAGTGGTTTGCC and 3′ end: ATTGACCTCAGAAGATGAACTC) obtained from Invitrogen. The 900 base-pair PCR product was then separated on a 1% agarose gel and purified using the QIAquick Gel Extraction Kit (Qiagen, Valencia, CA). Purified rat osteopontin cDNA was cloned into pCRII TOPO cloning vector and transfected into One Shot Top10 Chemically Competent *E.coli* (both from Invitrogen). Selected bacterial colonies were cultured and the plasmid DNA extracted using a modified STET boiling Mini-Prep protocol with lysozyme (STET buffer: 8% sucrose, 0.5% Triton X-100, 50 mM Tris pH 8.0, 50 mM EDTA). The sequence and directionality of cloned inserts was confirmed by PCR and direct sequencing (Boston University Genomics Department), and further amplified by large-preparation plasmid purification with EndoFree Plasmid Maxi Kit

(Qiagen). Finally, an antisense rat osteopontin DIG-labeled RNA probe was generated using the DIG RNA labeling Kit (SP6/T7) (Roche Applied Sciences, Minneapolis, MN) per the manufacturer's protocol.

Equalization of RNA loading on Northern blots was assessed by probing for beta-actin (Roche) and ribosomal 28S RNA. The r28S DIG-RNA probe was generated using a custom designed anti-sense oligonucleotide from Invitrogen (5′-ACCGATGAGAGTAGTGGTATTT-CACCG-3′) and then labeled with the DIG Oligonucleotide 3′-End Labeling Kit, 2nd Generation (Roche) per the manufacturer's protocol. Equal amounts of RNA were separated on a 1.0% agarose-formaldehyde gel in Northern-Max Formaldehyde Load Dye (Ambion, Inc., Austin, TX). RNA integrity was assessed by ethidium bromide gel staining (Sigma) for ribosomal 18S and 28S. RNA was then capillary-transferred overnight to a positive-charged nylon membrane (Roche) and fixed by Stratagene UV Cross-linker (Stratagene, La Jolla, CA). Blots were then incubated overnight in DIG Easy Hyb hybridization reagent (Roche) at 68 degrees C in 100 ng/ml of anti-rat osteopontin DIG-RNA probe. Blots were washed and re-probed overnight at 54°C with 1 μM of r28S DIG-oligo prior to developing using the DIG Detection Kit (Roche) per the manufacturer's protocol. Osteopontin mRNA expression was quantified by comparing the osteopontin and r28S signals by densitometry (ChemiImager System and AlphaEase software, Alpha Ionotech, San Leandro, CA).

Quantification of osteopontin mRNA expression was also determined using real-time PCR (qRT-PCR). Total RNA (1 μg) was reverse transcribed by 10 μg/μl M-MLV reverse transcriptase (Promega) with 5 μM of Oligo $dT_{18}$ (IDT) in a final volume of 20 μl. The reaction mixture also contained 1 μg/μl RNase inhibitor (Promega), M-MLV 5× RT Buffer (Promega) and 1.2 mM dNTP (Promega). Incubation cycles for the reverse transcriptase step were: 75°C for 3 min, 4°C for 10 min, 42°C for 60 min followed by 95°C for 3 min. The reactions were carried out in the PTC-150 minicycler. In brief, qRT-PCR was performed in an ABI PRISM 7700 sequence detector (Perkin Elmer/Applied Biosystems) in a final volume of 25 μl. The PCR mixture contained 0.2 μl cDNA and 12.5 μl of 2×TaqMan® Universal Master Mix (Applied Biosystems, ABI, Foster City, CA). Rat osteopontin-specific primer pair and TaqMan® probes were obtained from Applied Biosystems; GAPDH was used as a loading control (ABI). All genes were amplified by a first step of 15 s at 95°C followed by 1 min at 60°C for 40 cycles. The results were interpreted by the comparative $C_T$ method ($\Delta\Delta C_T$) for relative quantification of gene expression.

### Protein Analysis

Medium from rat LIC were centrifuged at 2,000*g* and the supernatants removed for assessment of secreted osteopontin protein. Fibroblast whole-cell lysates were prepared after twice washing the cells with cold PBS and extracting cellular proteins with ice-cold modified RIPA buffer (50 mM Tris-HCl, pH 7.4, 1% NP-40, 0.25% Na-deoxycholate, 150 mM NaCl, and 1 mM EDTA, PMSF, $Na_3VO_4$, and NaF each). Cells were homogenized, incubated for 15 min in lysis buffer and centrifuged at 14,000*g* at 4°C for 15 min. Protein concentration from cell lysate supernatant was measured by Bradford Assay with Bio-Rad Protein Assay (BioRad, Hercules, CA). Equal concentrations of protein were separated on 10% SDS–PAGE gel prior to transfer to nitrocellulose membrane (BioRad) and confirmed by Coomassie Brilliant Blue (BioRad) gel staining. Efficiency of protein transfer was evaluated by Ponceau S staining (Sigma). Membranes were then rinsed in distilled water, blocked for one hour at room temperature, and incubated overnight at 4°C in blocking buffer with diluted primary antibody.

Western blotting and ELSIA were used to assess osteopontin protein production. For detection of rat osteopontin by immunoblotting, we used a mouse monoclonal anti-rat osteopontin antibody MPIIIB10 (1 mcg/ml, Iowa Hybridoma Bank, University of Iowa) using conditions previously reported [Porter et al., 2002). In preliminary experiments, the MPIIIB10 antibody provided consistent and reliable detection of mouse recombinant and native rat osteopontin (data not shown). Mouse recombinant osteopontin derived from a mouse myeloma cell line (R&D) was used as a positive control (5 ng). Per the manufacturer's package insert, the apparent molecular weight of this highly glycosylated protein is 65 kD (calculated 31.5 kD) by SDS–PAGE under reducing conditions, similar to that described for native osteopontin. A horseradish peroxidase (HPR)-conjugated goat anti-mouse secondary antibody

(1:3,000 dilution, Pierce, Rockford, IL) was used for detection. Quantification of soluble rat osteopontin in cell culture supernatants was determined using a rat Osteopontin Enzyme Immunometric Assay Kit (TiterZyme EIA, Assay Designs, Inc., Ann Arbor, MI) per the manufacturer's protocol. This assay is specific for rat protein, having a $<0.01\%$ cross-reactivity for mouse or human osteopontin.

For assessment of MAPK signaling, immunoblotting was performed using rabbit polyclonal antibodies directed against total and phosphorylated ERK1/2, p38 MAPK, and JNK (all 1:1,000 dilution) followed by HRP-conjugated goat anti-rabbit secondary antibody (1:2,000, all obtained from Cell Signaling, Beverly, MA). Following stringency washes in all Western blotting experiments, SuperSignal West Pico Chemiluminescent Substrate (Pierce) was used for the immunodetection of selected proteins prior to autoradiograph exposure (Marsh Bio, Rochester, NY).

### Statistical Analysis

All statistics were performed on experiments repeated a minimum of three times, with a representative blot shown. Quantification of average mRNA expression was calculated from a minimum of three separate densitometry and/or qRT-PCR experiments. Results are expressed as a mean $\pm$ standard deviation (SD). Un-paired, two-tailed $t$-test was used for comparison of means. A $P$-value $= 0.05$ was considered significant for all statistical analyses.

## RESULTS

### Lung Fibroblasts Express Osteopontin in Response to Inflammatory and Pro-fibrotic Cytokines

We investigated whether the pro-fibrotic mediators found in the lung during the early inflammatory response to injury led to the expression of osteopontin in lung fibroblasts. Primary neonatal rat lung fibroblasts were cultured for 24 h with or without IL-1β, TNF-α, TGF-β, and AII. The amount of osteopontin mRNA was measured by Northern blot analysis (Fig. 1A). Resting lung fibroblasts expressed low levels of osteopontin mRNA. After IL-1β stimulation, osteopontin mRNA expression increased more than threefold over untreated fibroblasts (Fig. 1B, mean fold change $= 3.42 \pm 0.75$, $P = 0.03$ compared to untreated cells). TNF-α, TGF-β, and AII, all known contributors to injury-induced lung fibrosis, only minimally increased osteopontin expression in neonatal rat lung fibroblasts ($P > 0.05$ compared to untreated cells).

### Interleukin-1β Rapidly and Potently Induces Osteopontin mRNA Expression by Lung Fibroblasts

The kinetics of osteopontin expression after IL-1β treatment was examined. Cultured fibro-

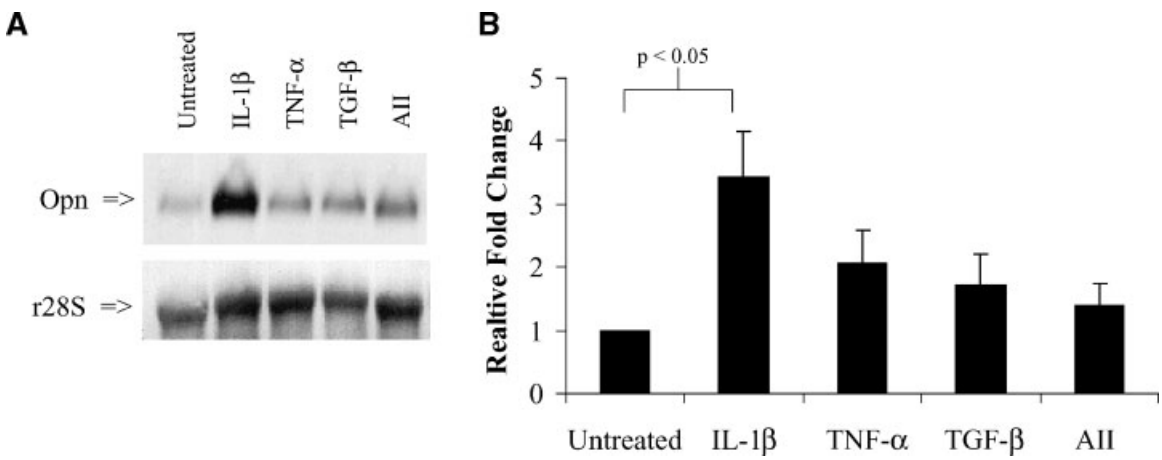


**Fig. 1.** Primary rat lung fibroblasts express osteopontin in response to pro-fibrotic mediators. **A**: Northern blot for rat osteopontin in primary rat lung fibroblasts 24 h after treatment with the pro-fibrotic mediators IL-1β (250 pg/ml), TNF-α (10 ng/ml), TGF-β (10 ng/ml), and AII ($10^{-5}$ M). Ribosomal 28S RNA was used as a loading control. Image shown is representative of three separate experiments. **B**: Histogram of densitometry normalized to r28S mRNA displaying fold-increase in osteopontin mRNA in untreated cells compared to treatment with IL-1β, TNF-α, TGF-β, and AII. The average relative fold change with standard deviations from three separate experiments is shown. Only the comparison between untreated and IL-1β treated cells was statistically different at a $P$-value $< 0.05$.

blasts treated with IL-1β for 0, 2, 4, 8, 16, and 24 h were harvested for total RNA and Northern blot analysis (Fig. 2A). Osteopontin steady-state mRNA increased slightly by 8 h and markedly by 16 h after IL-1β treatment. Osteopontin expression remained elevated at 24 h and up to 48 h after IL-1β treatment (data not shown). In order to demonstrate the requirement for IL-1 receptor engagement, IL-1β stimulated lung fibroblasts were pre-treated with or without a recombinant soluble IL-1 receptor antagonist (sIL-1ra). The naturally occurring anti-inflammatory sIL-1ra molecule binds to the IL-1 type 1 receptor but does not initiate signaling [Dinarello, 1997]. Northern blotting (Fig. 2B) demonstrates that the addition of sIL-1ra completely inhibited osteopontin expression in primary lung fibroblasts by IL-1β.

As both TNF-α and TGF-β are known to induce osteopontin expression, we also examined these mediators' dose and time-course responses by Northern blotting. Rat lung fibroblasts treated with increasing concentrations of TNF-α for 24 h led to dose-dependent increases in osteopontin expression (Fig. 2C), although TNF-α concentrations greater than 20 ng/ml led to cell toxicity. Lastly, rat lung fibroblasts treated with TGF-β demonstrated significant osteopontin mRNA expression but only after 48 h of treatment. This modest and delayed increase in native osteopontin message by TGF-β is consistent with prior studies [Noda et al., 1988).

### Interleukin-1β Induces Secretion of Soluble Osteopontin Protein by Lung Fibroblasts

We next examined by Western blotting protein from primary rat lung fibroblast culture supernatants and whole-cell lysates for the presence of extracellular (soluble) and cell-associated osteopontin, respectively (Fig. 3A). After 24 h of IL-1β treatment, there was a marked increase in soluble osteopontin found only in the cell culture supernatant. Post-translationally modified osteopontin protein was identified as a single band at approximately 65 kD by SDS–PAGE. No cell-associated (intracellular) 65 kD band was detected by immunoblotting with or without IL-1β treatment. In both conditions, two other bands at 54 and 90 kD were detected in the cell lysate fractions. Ritting and Feng [1998] previously described a non-specific 90 kD band; the lower molecular weight 54 kD band remains unidentified.

We next use a rat osteopontin immuno-assay (EIA) to confirm the specificity of the Western blotting findings and also quantify the amount of osteopontin secreted by rat lung fibroblasts (Fig. 3B). We found a greater than threefold increase in rat osteopontin protein in the culture supernatants from untreated and IL-1β treated cells (mean $3.15 \pm 0.16$), which correlated to an average concentration of rat osteopontin of 125 ng/ml after IL-1β stimulation.

### Interleukin-1β Regulates Osteopontin Expression Through the MAPK Pathways

IL-1β binding to its type-1 receptor causes coupling of the IL-1 receptor complex and activation of downstream signal transduction pathways, including members of the mitogen-activated protein kinase (MAPK) family (Dinarello, 1997]. Using specific inhibitors, we determined the selectivity of each MAPK pathway in IL-1β induced osteopontin expression (Fig. 4A and B). Changes in osteopontin mRNA were assessed from cells with and without IL-1β treatment in the presence of inhibitors to MAP kinase kinase (MEK), which functions upstream of extracellular-regulated protein kinases (ERK)1/2 (inhibitor compound U0126), p38 MAPK (SB203580), and c-Jun N-terminal kinase (JNK) (JNK inhibitor-I). The MEK inhibitor U0126 significantly inhibited osteopontin expression in the untreated rat lung fibroblasts ($26\% \pm 9$ decrease vs. medium alone, $P < 0.01$) and completely blocked its induction by IL-1β ($P > 0.1$ vs. untreated). In contrast, the p38 MAPK inhibitor SB203580 had no impact on basal osteopontin expression ($P > 0.05$) but partially suppressed the induction of osteopontin by IL-1β ($P = 0.02$). Finally, JNK inhibition blocked neither basal nor IL-1β-mediated osteopontin expression ($P > 0.5$ for both).

In order to confirm the participation of each MAPK pathway in IL-1β mediated signal transduction, we assessed by Western blotting the time course of activation for ERK1/2, p38 MAPK, and JNK in primary rat lung fibroblasts after IL-1β stimulation. Immunoblots for total and activated (phosphorylated) signaling intermediates are shown (Fig. 4C). IL-1β led to the phosphorylation of all three MAPK members, with maximum activation 15–30 min after treatment. Phosphorylation of both p42 and p44 MAPK (ERK 1 & 2, respectively) remained activated for up to 2 h post-treatment. In contrast to ERK1/2, p38 MAPK phosphorylation

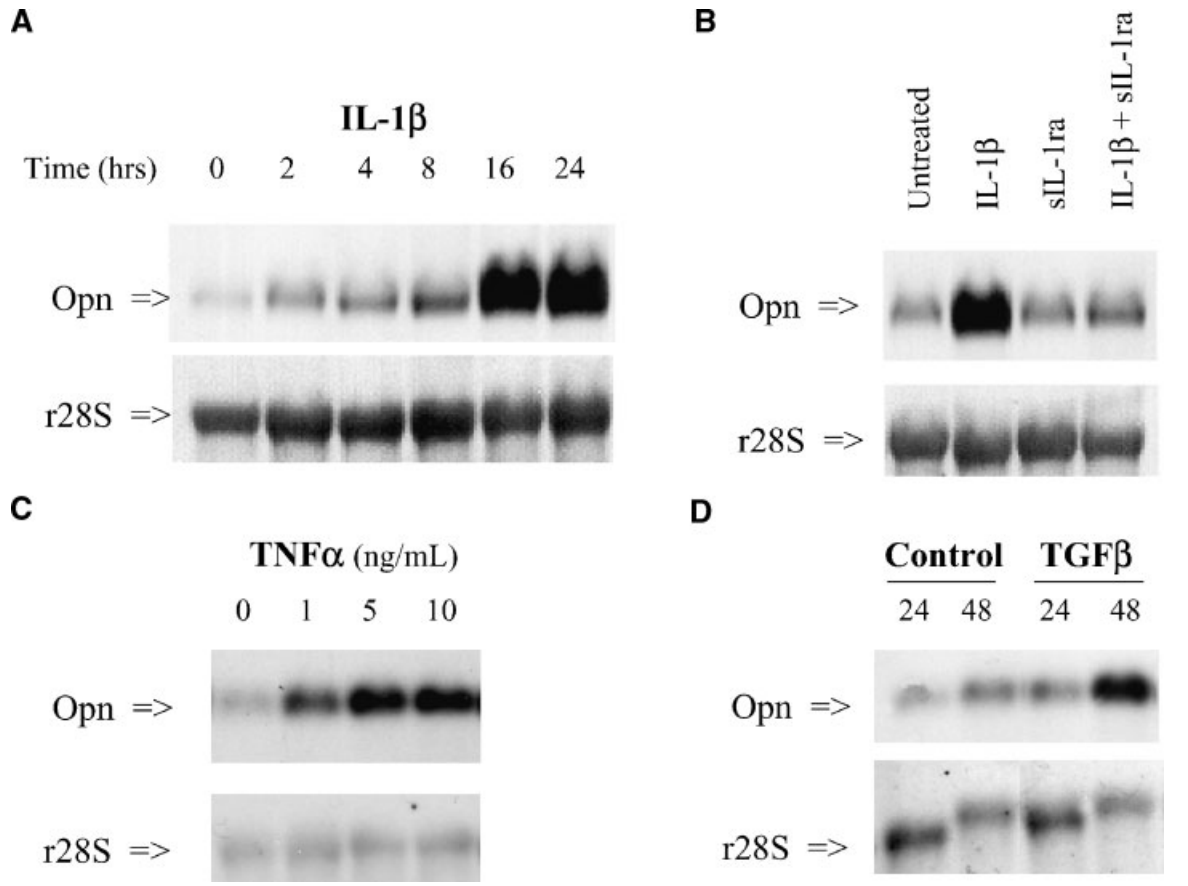


**Fig. 2.** IL-1β rapidly and potently induces osteopontin mRNA expression in rat lung fibroblasts. All panels show Northern blotting for rat osteopontin in treated primary rat lung fibroblasts. **A**: IL-1β (250 pg/ml) treatment for 0, 2, 4, 8, 16, and 24 h. **B**: Fibroblasts treated with or without IL-1β (250 pg/ml) and pre-treated with or without soluble IL-1 receptor antagonist (sIL-1ra, 150 ng/ml). **C**: Dose-response of osteopontin mRNA expression after 24 h of treatment with increasing concentrations of TNF-α (0, 1, 5, and 10 ng/ml). **D**: Fibroblasts in serum-free medium treated for 24 and 48 h in medium alone or TGF-β (10 ng/ml). Ribosomal 28S RNA is shown as a loading control in all panels. Northern blots shown are representative of at minimum two separate experiments.

was observed only transiently at 15–30 min after IL-1β treatment, quickly becoming inactive by 1 h. Lastly, we detected differential activation of the JNK isoforms by IL-1β. JNK1 (46 kD) was constitutively phosphorylated in the primary lung fibroblasts, but was further augmented by IL-1β treatment. The JNK2/3 (54 kD) isoforms (seen as a single band) only became phosphorylated upon IL-1β stimulation, but all the JNK isoforms reverted to their pre-treatment state 1-h post-IL-1β stimulation. No change in the amount of total protein was observed for any of the signaling proteins assayed.

Lastly, the efficiency of signaling inhibition was assessed by Western blotting for total and activated ERK1/2 after IL-1β treatment (Fig. 4D). The relative potency of PD98059 and U0126 to inhibit ERK1/2 phosphorylation was demonstrated, with moderate attenuation of ERK1/2 activation by PD98059 and complete inhibition by U0126, both in 10 μM concentrations. In summary, osteopontin expression in primary lung fibroblasts, both at unstimulated and after treatment with IL-1β, requires activation of ERK1/2, while p38 MAPK only modestly contributes to osteopontin induction by IL-1 β and JNK signaling not at all. All three MAPK pathways are activated upon IL-1β stimulation, yet they differentially contribute to the regulation of osteopontin in primary lung fibroblasts.

### Osteopontin mRNA Expression by IL-1β Requires de novo Transcription and Translation

In order to define further the mechanism responsible for osteopontin regulation by IL-1β, lung fibroblasts were pre-treated with actino-

mycin-D or cycloheximide, inhibitors of transcription, and translation, respectively (Fig. 5A and B). Induction of osteopontin mRNA by IL-1β was completely blocked in the presence of either of these inhibitors ($P > 0.3$ for all compared to untreated), suggesting the induction of osteopontin message by IL-1β requires both de novo transcription and translation. Along with the delayed kinetics of increased osteopontin message after IL-1β treatment, these findings suggest synthesis of an unidentified protein intermediate is required for osteopontin gene regulation by IL-1β.

## DISCUSSION

In these studies, we demonstrate for the first time that pulmonary fibroblasts express the multifunctional cytokine osteopontin. We find that IL-1β is a potent and early inducer of osteopontin expression in rat neonatal lung fibroblasts. This response requires signaling via the IL-1 receptor and leads to the secretion of soluble osteopontin protein. We show that IL-1β mediated osteopontin expression is dependent primarily upon signaling through the MAPK signaling pathway ERK1/2. Finally, regulation of osteopontin expression by IL-1β requires de novo gene transcription and protein synthesis.

Osteopontin is markedly upregulated in human fibrosing lung diseases, including idiopathic pulmonary fibrosis (IPF) and sarcoidosis [Zuo et al., 2002; O'Regan et al., 1999], as well as in multiple animal models of lung fibrosis [Nakama et al., 1998]. After bleomycin injury in mice, osteopontin mRNA levels increase with the onset of lung inflammation, but rise further and peak with the establishment of fibrosis [Takahashi et al., 2001]. Gene microarray studies on the β6-integrin-knockout mouse, which is protected from fibrosis after bleomycin lung injury, demonstrate attenuated osteopontin expression compared to wild-type animals despite the presence of extensive inflammation [Kaminski et al., 2000]. Based on these studies and others from the heart and kidney demonstrating osteopontin expression by interstitial fibroblasts, we postulated that lung interstitial cells are an important source of osteopontin during pulmonary fibroproliferation. In these studies, we show for the first time that primary lung fibroblasts produce osteopontin in response to inflammatory cytokines.

Primary neonatal rat lung fibroblasts were challenged with cytokines with known roles in the pathogenesis of pulmonary fibrosis and found in the milieu of the injured lung. We found that osteopontin expression is potently and selectively augmented by the inflammatory and pro-fibrotic cytokine IL-1β. In response to lung injury, such as that caused by acute

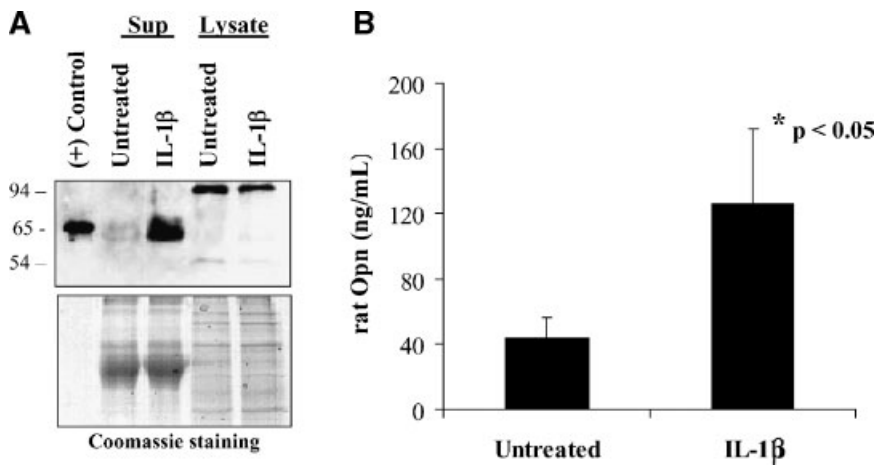


**Fig. 3.** IL-1β induces secretion of osteopontin protein from rat lung fibroblasts. **A**: A Western blot for rat osteopontin (MPIIIB10 primary antibody, 1:40 dilution) is shown. Protein from culture medium (Sup) and total cell lysates (lysate) were isolated from rat lung fibroblasts with or without IL-1β stimulation. Equal amounts of total protein were separated by gel electrophoresis. Recombinant, post-translationally modified mouse osteopontin (5 ng/lane) serves as a positive control seen at 65 kD on SDS–PAGE. Equal loading for cell supernatants and lysates is shown by Coomassie staining. **B**: Histogram of rat osteopontin concentration (ng/ml) as determined by rat osteopontin EIA from cell culture supernatants 24 h after treatment with medium alone (untreated) or IL-1β. Sample dilutions of 1:10, 1:100, and 1:1,000 were required given the high sensitivity of this assay (19.5 pg/ml). The mean ± SD from three separate experiments is shown.

respiratory distress syndrome (ARDS) and bleomycin, large amounts of IL-1β are produced [Kelly et al., 2003]. Experimentally, local overproduction of IL-1β using an intra-tracheally administered adenoviral vector leads to lung inflammation and marked pulmonary fibrosis [Kolb et al., 2001]. Furthermore, the co-administration of a soluble interleukin-1 receptor antagonist along with bleomycin attenuates the fibrogenic response in the lung to toxic injury, lending further evidence for the importance of IL-1β in the pathogenesis of injury-mediated lung fibrosis [Piguet et al., 1993].

After administration of intratracheal bleomycin, increased IL-1β message and protein are seen within 8 and 15 h, respectively. IL-1β production, primarily by alveolar macrophages, continues to increase at 3 days but by 1 week its production attenuates [Jordana et al., 1988; Cavarra et al., 2004]. The kinetics of osteopontin expression follows that of IL-1β. Osteopontin mRNA and protein are first detected 3 days after bleomycin challenge and increase further by 7 and 14 days [Nakama et al., 1998; Takahashi et al., 2001]. Thus, in the bleomycin model of inflammation-induced lung fibrosis,

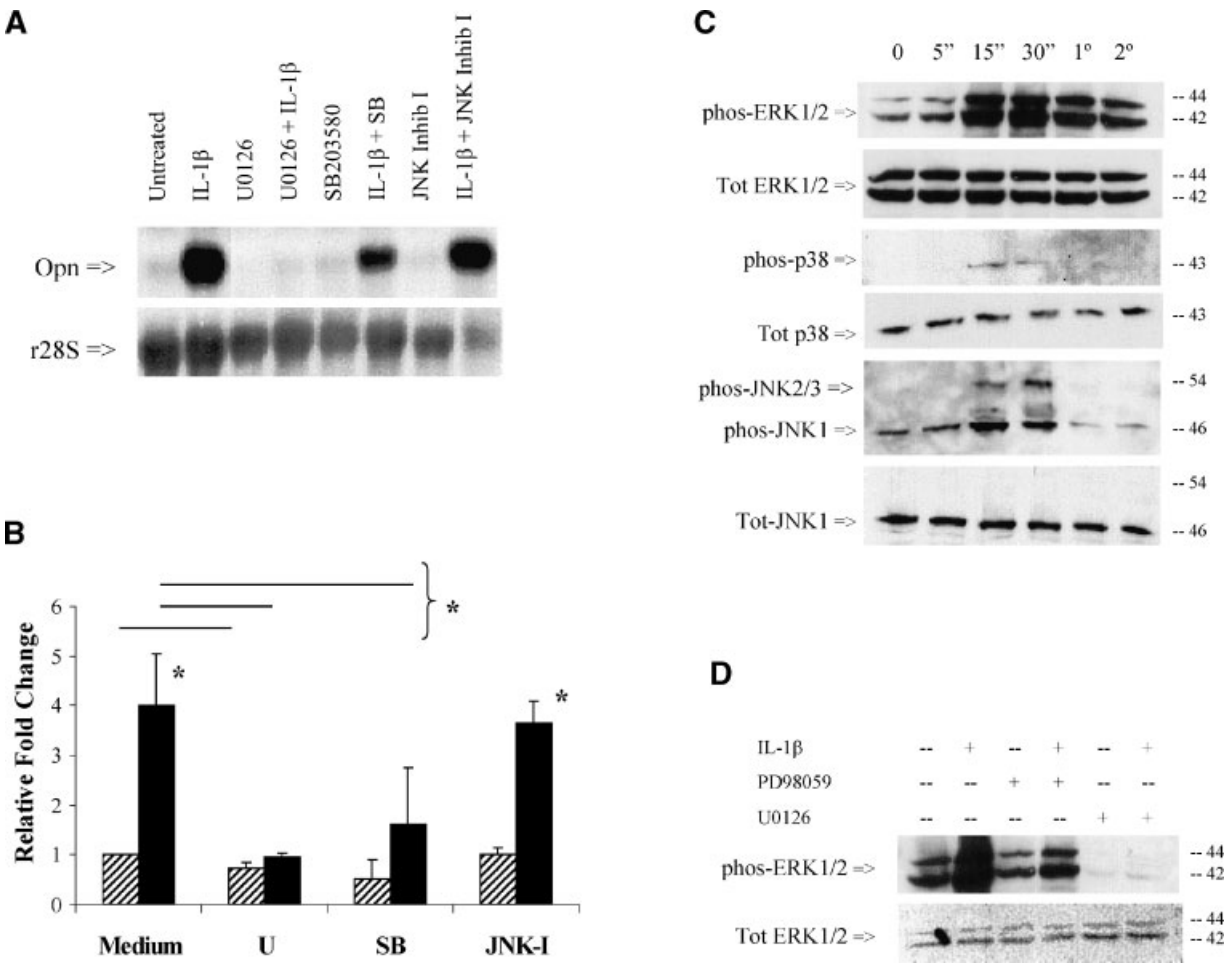


**Fig. 4.** MAPK signaling pathways mediate osteopontin expression by IL-1β. **A**: Northern blot of osteopontin from rat lung fibroblasts treated for 24 h with or without IL-1β (250 pg/ml) in the presence of the chemical inhibitors U0126, SB2003580, or JNK inhibitor peptide-I (all at concentrations of 10 μM). Ribosomal 28S RNA is shown as a loading control. **B**: Histogram of the mean ± SD relative fold-change in osteopontin mRNA for the conditions in (A) above. Grey bars represent untreated where black bars represent IL-1β treatment. Comparisons denoted with an asterisk (*) indicate statistical significance at a *P*-value $\leq 0.05$ for a minimum of three separate experiments. **C**: Western blotting for total and activated (phosphorylated) ERK1/2, p38 MAPK, and JNK from whole-cell lysates of rat lung fibroblasts 5 min to 2 h after treatment with IL-1β (250 pg/ml). Blotting for the non-phosphorylated isoforms demonstrates equal loading of protein per lane. **D**: Immunoblotting for total and phosphorylated ERK1/2 after 15 min with or without IL-1β treatment in the presence of the MEK1/2 inhibitors PD98059 and U0126 (both used at 10 μM). All immunoblots are representative of at least two separate experiments.

early IL-1β expression after tissue injury is temporally followed by induction of osteopontin, providing plausible in vivo evidence of osteopontin as a downstream effector of IL-1β.

We found that IL-1β stimulation of lung fibroblasts results in a receptor-dependent induction of osteopontin message and protein production with secretion of osteopontin into the extracellular space. Soluble osteopontin can function as an autocrine or paracrine cytokine [Rittling et al., 2002], affecting cellular migration, proliferation, and cell–matrix interactions [Ashizawa et al., 1996; Bendeck et al., 2000]. Osteopontin is a potent chemotactic factor for macrophages and smooth muscle cells [Bendeck et al., 2000], and augments the mitogenic effect of platelet-derived growth factor (PDGF) on murine 3T3 and human lung fibroblasts [Takahashi et al., 2001]. IL-1β, which we herein demonstrate is a potent inducer of extracellular osteopontin, also increases the expression of PDGF receptor-α on lung fibroblasts [Wang et al., 2000]. Thus, osteopontin may enhance the fibrotic stimulus initiated by IL-1β after lung injury through a positive feedback loop consisting of increased soluble osteopontin in concert with an increased responsiveness to PDGF.

We previously demonstrated that after bleomycin lung injury, osteopontin-deficient mice develop enlarged cystic airspaces along with decreased collagen type-1 expression, total MMP-2 production, and activated TGF-β [Berman et al., 2004]. Similar findings of abnormal tissue repair were seen in the skin and heart of osteopontin-deficient mice after injury [Liaw et al., 1998; Trueblood et al., 2001]. We also have shown that recombinant osteopontin in vitro can increase total and activated TGF-β and MMP-2 in both primary bronchial epithelial cells and a monocytic cell line [Li et al., 2003; Serlin et al., 2003]. One potential mechanism by which osteopontin may function "upstream" of TGF-β was suggested by recent data demonstrating the contribution of integrin $\alpha_v\beta_3$ ligation to TGF-β signaling and myofibroblast differentiation [Thannickal et al., 2003; Scaffidi et al., 2004]. Many of the cytokine functions attributed to osteopontin depend upon integrin $\alpha_v\beta_3$ ligation. Osteopontin, via signaling through integrin $\alpha_v\beta_3$, was shown to mediate AII-dependent myocardial fibroblast proliferation and collagen gel contraction [Ashizawa et al., 1996]. Furthermore, osteopontin can bind collagens I and III in vitro, and this interaction is enhanced by the formation of osteopontin multimers by tissue transglutaminases [Kaartinen et al., 1999]. Taken together, we propose a model whereby fibroblast-derived osteopontin functions in an autocrine and/or paracrine manner to increase cellular proliferation and augment ECM remodeling within the injured lung.

The mechanism of osteopontin regulation by IL-1β in fibroblasts has not been well defined. IL-1β treatment of periodontal fibroblasts leads to secretion of soluble, non-matrix associated osteopontin into the extracellular space [Chien et al., 1999]. In primary rat myocardial fibroblast, IL-1β augments AII-dependent increases in osteopontin message and protein [Xie et al.,

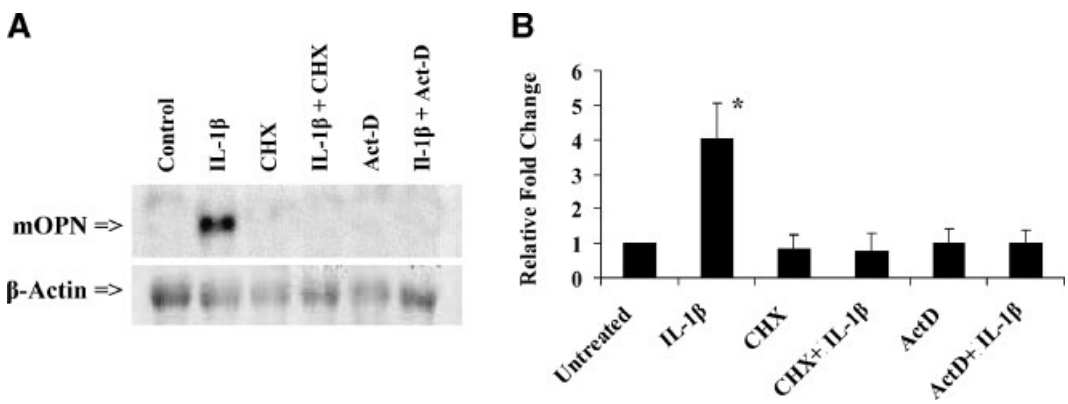


**Fig. 5.** IL-1β regulation of osteopontin expression in primary rat lung fibroblasts requires de novo transcription and translation. **A**: Northern blot for osteopontin from rat lung fibroblasts after 24 h with or without IL-1β treatment (250 pg/ml) and in the presence of cycloheximide (10 μg/ml) or actinomycin-D (1 μg/ml). β-actin is shown as a loading control. **B**: Histogram of the average ± SD relative fold-changes in osteopontin mRNA for the conditions in (A). The asterisk (*) indicates statistical significance at a *P*-value = 0.01 for a minimum of three separate experiments comparing untreated to IL-1β treatement. No other conditions were statistically significantly different from the untreated control.

2004]. This is in contrast to our findings in lung fibroblasts, where we demonstrate that IL-1β alone is sufficient for inducing osteopontin expression. IL-1β activates all three MAPK pathways: MEK, p38 MAPK, and JNK. Induction of osteopontin in myocardial fibroblasts is mediated through activation of the signal transduction pathways ERK1/2 and JNK but not p38 MAPK. However, in primary rat lung fibroblasts, we find osteopontin induction by IL-1β is dependent upon activation of ERK1/2 and p38 MAPK, but not JNK. Our studies also indicate that induction of osteopontin mRNA by IL-1β requires synthesis of protein intermediates, as suggested by the delayed time-course of osteopontin expression after IL-1β stimulation and the inhibitory effects of actinomycin-D and cycloheximide. Defining the intermediary steps in the regulation of fibroblast-derived osteopontin could lead to the further identification of downstream elements contributing to IL-1β-mediated lung fibrosis.

In summary, our data support the hypothesis that lung fibroblasts contribute to the increased osteopontin expression observed in pulmonary fibrosis. We demonstrate that IL-1β is a potent and selective inducer of osteopontin message and protein in lung fibroblasts. Osteopontin regulation by IL-1β is dependent upon activation of the MAPK signaling pathway and de novo transcription and translation. Previous studies by our lab and others have shown increased macrophage and epithelial osteopontin expression after lung injury [Takahashi et al., 2001; Berman et al., 2004]. We now propose that fibroblasts serve as a source of osteopontin during lung fibroproliferation. The form, timing, and cellular source of osteopontin during the reparative response likely determines its ultimate role in mediating wound healing and lung remodeling after injury. Further elucidating the signaling and transcriptional regulation of osteopontin in lung fibroblasts will enhance our understanding of the complex network of cytokines, growth factors, and extracellular matrix components that together contribute to the pathogenesis of pulmonary fibrosis.

## ACKNOWLEDGMENTS

The authors thank David Rishikof for his insightful comments and review of the manuscript. This study was supported by NIH/NHLBI grant numbers F32-HL71388 (to D.M.S.), R01-HL63339 (to J.S.B.) and R01-HL70182, P01-HL46902 (to R.H.G.).

## REFERENCES

Ashizawa N, Graf K, Do YS, Nunohiro T, Giachelli CM, Meehan WP, Tuan TL, Hsueh WA. 1996. Osteopontin is produced by rat cardiac fibroblasts and mediates A(II)-induced DNA synthesis and collagen gel contraction. J Clin Invest 98:2218–2227.

Bendeck MP, Irvin C, Reidy M, Smith L, Mulholland D, Horton M, Giachelli CM. 2000. Smooth muscle cell matrix metalloproteinase production is stimulated via alpha(v)beta(3) integrin. Arterioscler Thromb Vasc Biol 20:1467–1472.

Berman JS, Serlin D, Li XF, Whitley G, Hayes J, Rishikof DC, Ricupero DA, Liaw L, Goetschkes M, O'Regan AW. 2004. Altered bleomycin-induced lung fibrosis in osteopontin-deficient mice. Am J Physiol Lung Cell Mol Physiol 286:L1311–L1318.

Carreras I, Rich CB, Jaworski JA, DiCamillo SJ, Panchenko MP, Goldstein R, Foster JA. 2001. Functional components of basic fibroblast growth factor signaling that inhibit lung elastin gene expression. Am J Physiol Lung Cell Mol Physiol 281:L766–L775.

Cavarra E, Carraro F, Fineschi S, Naldini A, Bartalesi B, Pucci A, Lungarella G. 2004. Early response to bleomycin is characterized by different cytokine and cytokine receptor profiles in lungs. Am J Physiol Lung Cell Mol Physiol 287:L1186–L1192.

Chien HH, Lin WL, Cho MI. 1999. Interleukin-1 beta-induced release of matrix proteins into culture media causes inhibition of mineralization of nodules formed by periodontal ligament cells in vitro. Calcif Tissue Int 64: 402–413.

Dinarello CA. 1997. Interleukin-1*1. Cytokine Growth Factor Rev 8:253–265.

Jordana M, Richards C, Irving LB, Gauldie J. 1988. Spontaneous in vitro release of alveolar-macrophage cytokines after the intratracheal instillation of bleomycin in rats—Characterization and kinetic-studies. Am Rev Respir Dis 137:1135–1140.

Kaartinen MT, Pirhonen A, Linnala-Kankkunen A, Maenpaa PH. 1999. Cross-linking of osteopontin by tissue transglutaminase increases its collagen binding properties. J Biol Chem 274:1729–1735.

Kaminski N, Allard JD, Pittet JF, Zuo F, Griffiths MJD, Morris D, Huang X, Sheppard D, Heller RA. 2000. Global analysis of gene expression in pulmonary fibrosis reveals distinct programs regulating lung inflammation and fibrosis. PNAS 97:1778–1783.

Kelly M, Kolb M, Bonniaud P, Gauldie J. 2003. Re-evaluation of fibrogenic cytokines in lung fibrosis. Curr Pharm Des 9:39–49.

Kolb M, Margetts PJ, Anthony DC, Pitossi F, Gauldie J. 2001. Transient expression of IL-1 beta induces acute lung injury and chronic repair leading to pulmonary fibrosis. J Clin Invest 107:1529–1536.

Kuang PP, Goldstein RH. 2003. Regulation of elastin gene transcription by interleukin-1 beta-induced C/EBP beta isoforms. Am J Physiol-Cell Physiol 285:C1349–C1355.

Lan HY, Yu XQ, Yang NS, Nikolic-Paterson DJ, Mu W, Pichler R, Johnson RJ, Atkins RC. 1998. De novo glomerular osteopontin expression in rat crescentic glomerulonephritis. Kidney Int 53:136–145.

Li XF, Whitley G, Serlin DM, Liaw L, Berman JS, O'Regan A. 2003. Decreased expression of MMP-2 in osteopontin null mice during lung fibrosis. Am J Respir Crit Care Med 167:A192. [Abstract].

Liaw L, Birk DE, Ballas CB, Whitsitt JS, Davidson JM, Hogan BLM. 1998. Altered wound healing in mice lacking a functional osteopontin gene (*spp1*). J Clin Invest 101:1468–1478.

Miyazaki Y, Tashiro T, Higuchi Y, Setoguchi M, Yamamoto S, Nagai H, Nasu M, Vassalli P. 1995. Expression of osteopontin in a macrophage cell-line and in transgenic mice with pulmonary fibrosis resulting from the lung expression of a tumor-necrosis-factor-alpha transgene. Osteopontin: Role Cell Signal Adhes 760:334–341.

Nakama K, Miyazaki Y, Nasu M. 1998. Immunophenotyping of lymphocytes in the lung interstitium and expression of osteopontin and interleukin-2 mRNAs in two different murine models of pulmonary fibrosis. Exp Lung Res 24:57–70.

Noda M, Yoon K, Prince CW, Butler WT, Rodan GA. 1988. Transcriptional regulation of osteopontin production in rat osteosarcoma cells by type beta transforming growth factor. J Biol Chem 263:13916–13921.

O'Regan A. 2003. The Role of osteopontin in lung disease. Cytokine Growth Factor Rev 14:479–488.

O'Regan AW, Chupp GL, Lowry JA, Goetschkes M, Mulligan N, Berman JS. 1999. Osteopontin is associated with T cells in sarcoid granulomas and has T cell adhesive and cytokine-like properties in vitro. J Immunol 162:1024–1031.

O'Regan AW, Nan GJ, Chupp GL, Berman JS. 2000. Osteopontin (Eta-1) in cell-mediated immunity: Teaching an old dog new tricks. Immunol Today 21:475–478.

O'Regan AW, Hayden JM, Body S, Liaw L, Mulligan N, Goetschkes M, Berman JS. 2001. Abnormal pulmonary granuloma formation in osteopontin-deficient mice. Am J Respir Crit Care Med 164:2243–2247.

Persy VP, Verhulst A, Ysebaert DK, De Greef KE, De Broe ME. 2003. Reduced postischemic macrophage infiltration and interstitial fibrosis in osteopontin knockout mice. Kidney Int 63:543–553.

Piguet PF, Vesin C, Grau GE, Thompson RC. 1993. Interleukin-1 receptor antagonist (Il-1Ra) prevents or cures pulmonary fibrosis elicited in mice by bleomycin or silica. Cytokine 5:57–61.

Porter JD, Khanna S, Kaminski HJ, Rao JS, Merriam AP, Richmonds CR, Leahy P, Li JJ, Guo W, Andrade FH. 2002. A chronic inflammatory response dominates the skeletal muscle molecular signature in dystrophin-deficient mdx mice. Hum Mol Genet 11:263–272.

Ritting SR, Feng F. 1998. Detection of mouse osteopontin by western blotting. Biochem Biophys Res Commun 250:287–292.

Rittling SR, Chen YP, Feng F, Wu YM. 2002. Tumor-derived osteopontin is soluble, not matrix associated. J Biol Chem 277:9175–9182.

Scaffidi AK, Petrovic N, Moodley YP, Fogel-Petrovic M, Kroeger KM, Seeber RM, Eidne KA, Thompson PJ, Knight DA. 2004. Alpha(v)beta(3) integrin interacts with the transforming growth factor beta (TGF beta) type II receptor to potentiate the proliferative effects of TGF beta 1 in living human lung fibroblasts. J Biol Chem 279:37726–37733.

Serlin DM, Whitley G, Li XF, Rishikof DC, Ricupero DA, Hayes J, Berman JS, O'Regan A. 2003. Osteopontin regulates type-1 collagen and TGF-b expression in bleomycin induced lung fibrosis. Am J Respir Crit Care Med 167:A350. [Abstract].

Takahashi F, Takahashi K, Okazaki T, Maeda K, Ienaga H, Maeda M, Kon S, Uede T, Fukuchi Y. 2001. Role of osteopontin in the pathogenesis of bleomycin-induced pulmonary fibrosis. Am J Respir Cell Mol Biol 24:264–271.

Thannickal VJ, Lee DY, White ES, Cui Z, Larios JM, Chacon R, Horowitz JC, Day RM, Thomas PE. 2003. Myofibroblast differentiation by transforming growth factor-beta 1 is dependent on cell adhesion and integrin signaling via focal adhesion kinase. J Biol Chem 278:12384–12389.

Trueblood NA, Xie Z, Communal C, Sam F, Ngoy S, Liaw L, Jenkins AW, Wang J, Sawyer DB, Bing OHL, Apstein CS, Colucci WS, Singh K. 2001. Exaggerated left ventricular dilation and reduced collagen deposition after myocardial infarction in mice lacking osteopontin. Circ Res 88:1080–1087.

Wang YZ, Zhang P, Rice AB, Bonner JC. 2000. Regulation of interleukin-1 beta-induced platelet-derived growth factor receptor-alpha expression in rat pulmonary myofibroblasts by p38 mitogen-activated protein kinase. J Biol Chem 275:22550–22557.

Xie ZL, Singh M, Singh K. 2004. ERK1/2 and JNKs, but not p38 kinase, are involved in reactive oxygen species-mediated induction of osteopontin gene expression by angiotensin II and interleukin-1 beta in adult rat cardiac fibroblasts. J Cell Physiol 198:399–407.

Yu XQ, Fan JM, Nikolic-Paterson DJ, Yang N, Mu W, Pichler R, Johnson RJ, Atkins RC, Lan HY. 1999. IL-1 up-regulates osteopontin expression in experimental crescentic glomerulonephritis in the rat. Am J Pathol 154:833–841.

Zohar R, Suzuki N, Suzuki K, Arora P, Glogauer M, McCulloch CA, Sodek J. 2000. Intracellular osteopontin is an integral component of the CD44-ERM complex involved in cell migration. J Cell Physiol 184:118–130.

Zuo F, Kaminski N, Eugui E, Allard J, Yakhini Z, Ben Dor A, Lollini L, Morris D, Kim Y, DeLustro B, Sheppard D, Pardo A, Selman M, Heller RA. 2002. Gene expression analysis reveals matrilysin as a key regulator of pulmonary fibrosis in mice and humans. PNAS 99: 6292–6297.